

discussions in ref 2f and 12). In the limit where zero-frequency terms dominate and motions are highly anisotropic, if $J_{\text{CH}}(0) \sim {}^4/9 J_{\text{CSA}}(0)$ (i.e., $\gamma_{\text{C}}\gamma_{\text{H}}\hbar r_{\text{CH}}^{-3} \sim {}^2/3 \omega_{\text{C}}\Delta\sigma$), then $(1/T_2)_+/(1/T_2)_- \sim \infty$. In the present case, $(1/T_2)_+/(1/T_2)_- \sim 1.4 \pm 0.2$, indicating $\gamma_{\text{C}}\gamma_{\text{H}}\hbar r_{\text{CH}}^{-3} \sim 8\omega_{\text{C}}\Delta\sigma$. Therefore, the approximate magnitude of the methyl carbon CSA is 60 ± 20 ppm. Since nonsecular terms may not be entirely negligible, this value for $\Delta\sigma$ should be considered as a lower limit. Liquid-crystalline and solid-state studies yield values in the range 65 ± 15 ppm.²²

In the limit where $J_{\text{CH}} = J_{\text{HCH}}$ and adiabatic terms dominate, the central two lines of the methyl quartet are Lorentzian with

$$\left(\frac{1}{T_2}\right)_{\pm}^{\text{inner}} = \frac{8}{3}J_{\text{CSA}}(0) + \frac{2}{3}J_{\text{CH}}(0) = \frac{8}{3}J_{\text{CSA-D}}(0)$$

Although this limit does not strictly obtain, it is apparent from Figure 1 that the central lines are narrowed relative to the outer lines because of the diminished importance of carbon-hydrogen dipolar interactions. Furthermore, the differential broadening between the two central components is more pronounced than the differential broadening between the two outer components, once again in agreement with theory.

It is remarkable that dipolar-CSA cross correlations are clearly important even though $J_{\text{CH}}(0) \sim 60J_{\text{CSA}}(0)$. It has been noted elsewhere²³ that utilization of relaxation-induced multispin order may make it possible to observe anisotropic spin interactions that are intrinsically 3 or 4 orders of magnitude weaker than a dominant, temporally correlated interaction. This realization has exciting implications and awaits exploitation.

Conclusions

This relaxation study indicates that the magnetic relaxation behavior of adsorbed methanol is dominated by highly anisotropic motions. At least one characteristic motion is long on a time scale compared with $1/\omega_{\text{C}}$, whereas another motion (presumably rotation about the $-\text{CH}_3$ axis) is short compared to $1/\omega_{\text{C}}$. This is consistent with a model of methanol that is hydrogen bonded to either siloxane or free silanol. The silanol functionality has been shown¹⁷ to predominate in silicas treated at 250 °C. The presence

(22) (a) Pines, A.; Gibby, M.; Waugh, J. S. *Chem. Phys. Lett.* **1972**, *15*, 373. (b) Strub, H.; Beeler, A. J.; Grant, D. M.; Michl, J.; Cutts, P. W.; Zilm, K. W. *J. Am. Chem. Soc.* **1983**, *105*, 3333.

(23) Werbelow, L. G.; Allouche, A.; Pouzard, G. *J. Chem. Soc., Faraday Trans. 2* **1987**, *83*, 871.

of these hydroxyl groups is consistent with the proton relaxation data presented above. Future studies will investigate the effects of higher temperature treatment of the sol-gel silica on the relaxation behavior of adsorbed methanol.

Studies²⁴ in this laboratory have shown that at lower methanol loading, cross-polarization spectra reveal a broad and narrow component with different T_1 and T_{CH} values. At the loading levels of the current experiment the broad spectral component is not evident. The implication, however, is that there exists at low abundance at least one methanol species that experiences a strong proton dipole-coupling.

The argument has been made that interference or cross-correlation effects such as those described in this work provide a detailed description of molecular dynamics and anisotropic interaction at the molecular level. The relative magnitudes of dipolar and CSA interactions as well as the degree of dipolar-dipolar and dipolar-CSA cross correlation have been determined from relatively straightforward relaxation studies performed at a single field strength. Cross correlations and the manifestation of cross-correlation multispin order can be used to determine absolute signs of various spin couplings and position the principal axes of spin interaction. Most importantly, the evolution of multispin order is extremely sensitive to motional anisotropies and can be used to investigate highly anisotropic systems where conventional NMR relaxation studies would fail.

The studies and analyses described in this work do not exhaust the informational content of temporal correlation of anisotropic spin interaction. Experiments in progress include (i) the use of complementary pulse perturbations that selectively explore additional cross-correlation factors, (ii) studies involving the selective creation and dissipation of four-spin order, and (iii) the application of multiquantum relaxation that probes alternative manifestations of multispin order and cross correlation. It is anticipated that dynamic correlation NMR spectroscopy will become the method of choice in the study of dynamic structure.

Acknowledgment. We acknowledge Los Alamos National Laboratory Director's Funded Postdoctoral Fellowships for support of C.J.H. and P.C.S. This work was supported by the U.S. Department of Energy under Contract No. W-7405 ENG-86.

Registry No. Methanol-¹³C, 14742-26-8.

(24) Hartzell, C. J.; Lynch, T. J.; Earl, W. E., unpublished work.

Study of ³¹P NMR Chemical Shift Tensors and Their Correlation to Molecular Structure

Sun Un^{†,‡} and Melvin P. Klein^{*‡}

Contribution from the Department of Chemistry and Chemical Biodynamics Division, Lawrence Berkeley Laboratory, University of California, Berkeley, Berkeley, California 94720.

Received October 13, 1988

Abstract: The nature of the ³¹P anisotropic chemical shift interaction is examined by using magic-angle sample spinning NMR. Linear correlations between the principal values of the ³¹P chemical shift tensor, P-O bond lengths, and O-P-O bond angles are established. On the basis of a previously established correlation between P-O bond length and d_{P-P_O} π-bond order, values of the ³¹P chemical shift tensor elements were determined to be linearly related to d_{P-P_O} π-bond order. Furthermore, from correlations between bond lengths and bond angles, it was concluded that for the phosphates reported in this study the π- and σ-bond contributions to the ³¹P chemical shift interaction are not independent of each other and, hence, cannot be separated into distinct terms. A review of other phosphoryl derivatives suggests that these observations may be general for other quadruply coordinated phosphorus compounds.

More than 20 years ago, Lechter and Van Wazer¹ identified three factors that determined the changes in ³¹P isotropic chemical

shifts. The equation

$$\Delta\delta = a\Delta n_{\pi} - b\Delta\chi + c\Delta\theta_{\sigma} \quad (1)$$

compactly summarizes their findings, where a , b , and c are con-

[†]Department of Chemistry.

[‡]Chemical Biodynamics Division.

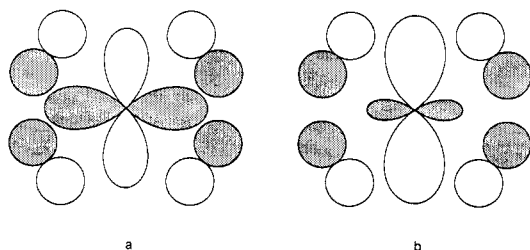


Figure 1. The two d-p π -bonding orbitals: (a) overlap of the $P(3d_{x^2-y^2})$ with 4 $O(2p)$ and (b) overlap of the $P(3d_{z^2})$ with 4 $O(2p)$.

stants and n_π is the π -bond order, χ is the electronegativity of the substituent, θ_σ is the σ -bond angle, and finally δ is the chemical shift. The relative importance of each of the three contributions has been under some debate.² Recent data indicate that the O-P-O bond angles play a predominant role in determining differences in the isotropic chemical shifts.²⁻⁴

Most of the experimental and theoretical studies have been limited to the isotropic part of the chemical shift interaction, while only a few have exploited its tensorial nature. Dutasta⁵ has studied the cyclic thioxophosphonates and a phosphane oxides, sulfides, and selenides. A linear relationship between the asymmetry parameter and the intracyclic O-P-O bond angles of the cyclic thioxophosphonates was found. Grimmer⁶ observed a linear relationship between the chemical shift anisotropy, $\Delta\sigma = \sigma_{||} - \sigma_{\perp}$, and the P-O bond length of various compounds of the form POX_3 ($X = F, Cl, Br, \text{ and methyl}$) all of which are axially symmetric. More recently, Turner⁷ has empirically correlated the chemical shifts of orthophosphates with the electronegativity and the cationic radius of the counterion. They also found correlations between the chemical shift anisotropy and average deviation of the O-P-O bond angle from the tetrahedral value.

A direct comparison of structural parameters, such as bond lengths and angles, and the ^{31}P chemical shift tensors has not yet been reported. To understand why a relationship between the principal values of the chemical shift tensor and molecular structure exists, we first qualitatively summarize the relationship between the length of P-O bonds and the extent of d_p-p_O π character of these bonds which was first discussed by Cruickshank.⁸ The two relevant P-O d_p-p_O π bonds are shown in Figure 1. With increase in the d_p-p_O π -bond order, the bond length of a given P-O bond is expected to decrease. Ester bonds of the type P-OR (where R = P, C, H) are expected to be longer than simple P-O bonds. The presence of the addition R-O bond would reduce or eliminate the p-orbital contribution of the oxygen to the d_p-p_O π -bond. In fact, this relationship between P-O bond lengths and d_p-p_O π -bond order is linear.⁸ Hence, these observations along with those of Lechter and Van Wazer, summarized by eq 1, suggest that straightforward relationships should exist between the ^{31}P chemical shift interaction and P-O bond lengths. If both the structure and the chemical shift tensor were known, it would be possible to deduce the bonding effects of a particular P-O bond on the chemical shift interaction without limiting the analysis to the effect on the isotropic chemical shift value which is an average over all directions and, hence, over all P-O bonds. Similarly, the

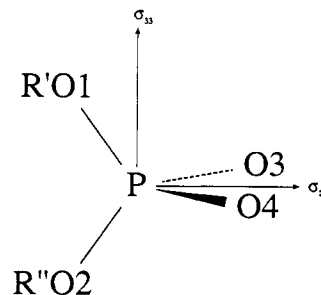


Figure 2. Orientation of the chemical shift tensor with respect to the molecular frame. The σ_{11} element is perpendicular to the elements shown and extends out toward the viewer. $R' = P, C, H$ and $R'' = P, C, H$.

dependence of the ^{31}P chemical shift interaction on the σ bonds might be deduced from bond-angle correlations.^{1,9}

Our approach was to measure and compile from the literature ^{31}P shift tensors of a variety of phosphates and phosphate esters. Comparisons between shift tensors and structures were facilitated by existing X-ray crystallographic data for most of the compounds. The chemical shift tensors were measured from ^{31}P NMR spectra detected by using magic-angle sample spinning (MASS). In addition to providing high resolution, MASS affords a straightforward means of measuring both the isotropic and anisotropic parts of the chemical shift interaction. A typical MASS spectrum consists of a set of resonances for each unique spin. These resonances appear centered about a peak the frequency of which corresponds to the isotropic chemical shift at integer multiples of the spinning frequency.¹⁰ The relative intensities of the isotropic peak and its spinning sidebands contain information from which the chemical shift tensor values can be determined. The detailed theoretical treatment of the recovery of the chemical shift tensor from MASS spectra has been given by Marciq and Waugh,¹⁰ who have used a moment analysis, and by Herzfeld and Berger,¹¹ who have calculated numerically the theoretical spinning sideband intensities.

To completely specify the chemical shift tensor, its orientation with respect to the molecular frame must also be established. From the single-crystal studies of Kohler¹² and of Herzfeld,¹³ it has been shown that the orientation of the ^{31}P chemical shift tensors of phosphates and phosphate esters are relatively constant and, more importantly, the principal axes of the tensors are oriented roughly along the P-O bond directions. In a MASS study of sodium triphosphate, Burlinson¹⁴ deduced the tensor orientations to be very similar to those cited above. The approximate orientation of the shift tensors that have been studied is shown in Figure 2. This orientation has been rationalized by Kohler¹² on the basis of the anticipated electron density around the phosphorus nuclei. We have assumed that this is the approximate tensor orientation of all of the phosphates and phosphate esters that are discussed in this paper.

Experimental Section

Materials. Sodium adenosine triphosphate (NaATP) was purchased from Sigma and used without further purification. The bis(2-pyridyl)amine (BPA) complexes of Mg- and CaATP were prepared by using the method of Cini.¹⁵ Equimolar quantities of the appropriate metal sulfate, 2,2'-dipyridylamine, and NaATP were mixed in 150 mL of 30% ethanol. The precipitate was washed with 30% ethanol followed by cold water. Sodium dihydrogen pyrophosphate was made by using a standard synthesis procedure.¹⁶ Sodium pyrophosphate anhydride was made by

(1) (a) Lechter, J. H.; Van Wazer, J. R. *Top. Phosphorus Chem.* **1967**, 75-226. (b) Lechter, J. H.; Van Wazer, J. R. *J. Chem. Phys.* **1965**, *44*, 815-829. (c) Constello, A. J. R.; Glonek, T.; Van Wazer, J. R. *Inorg. Chem.* **1976**, *15*, 972-974.

(2) (a) Gorenstein, D. G. *J. Am. Chem. Soc.* **1975**, *97*, 898. (b) Gorenstein, D. G. In *Phosphorus-31 NMR*; Gorenstein, D. G., Ed.; Academic Press: San Francisco, 1984; pp 7-36.

(3) Blackburn, G. M.; Cohen, J. S.; Weatherall, I. *Tetrahedron* **1971**, *27*, 2903-2912.

(4) Prado, F. R.; Geissner-Pretre, C.; Pullman, B.; Daudey, J.-P. *J. Am. Chem. Soc.* **1979**, *101*, 1737-1742.

(5) Dutasta, J. P.; Roberts, J. B.; Wiesenfeld, L. In *Phosphorus Chemistry*; Quin, L. D., Verade, J. G., Eds.; American Chemical Society: Washington, D.C., 1981.

(6) Grimmer, A. R. *Spectrochim. Acta* **1978**, *34a*, 941.

(7) Turner, G. L.; Smith, K. A.; Kirkpatrick, R. J.; Oldfield, E. *J. Magn. Reson.* **1986**, *70*, 408-415.

(8) Cruickshank, D. W. J. *J. Chem. Soc.* **1961**, 5486-5504.

(9) Huheey, J. E. *Inorganic Chemistry*; Harper: New York, 1978.

(10) Marciq, M. M.; Waugh, J. S. *J. Chem. Phys.* **1979**, *70*, 3300-3316.

(11) Herzfeld, J.; Berger, A. E. *J. Chem. Phys.* **1980**, *73*, 6021-6030.

(12) (a) Kohler, S. J.; Ellett, J. D.; Klein, M. P. *J. Chem. Phys.* **1976**, *50*, 4451-4452. (b) Kohler, S. J. Doctoral Thesis, University of California; Berkeley, 1975.

(13) Herzfeld, J.; Griffin, R. G.; Haberkorn, R. A. *Biochemistry* **1978**, *17*, 2711-2643.

(14) Burlinson, N. E.; Dunnell, B. A.; Ripmeister, J. A. *J. Magn. Reson.* **1986**, *67*, 217-230.

(15) Cini, R.; Burla, M. C.; Nunzi, A.; Polidori, G. P.; Zanazzi, P. F. *J. Chem. Soc., Dalton Trans.* **1984**, 2467-2476.

(16) Bell, R. N. *Inorg. Synth.* **1950**, *3*, 99-103.

Table I. ³¹P Chemical Shift Tensor Element Values^a

compound	σ_{33}	σ_{22}	σ_{11}	σ_{iso}
urea-phosphoric acid complex ^a	26.6	2.5	-44.6	-5.2
magnesium phosphate octahydrate	42.5	-27.2	-64.7	-16.5
sodium hydrogen phosphate dodecahydrate	55.4	-35.5	-69.8	-16.6
magnesium hydrogen phosphate trihydrate (newberyite)	48.0	-28.0	-67.8	-15.9
calcium hydrogen phosphate dihydrate (brushite) ²	70.0	-12.0	-53.0	-1.0
calcium dihydrogen phosphate monohydrate ^b				
(1)	49.0	1.0	-48.8	0.7
(2)	59.0	7.0	-66.0	0.0
barium diethylphosphate ^a	75.9	17.5	-109.8	-5.5
sodium GMP heptahydrate	70.2	-15.2	-37.9	5.7
phosphorylethanolamine ^{a,c}	68.6	-12.0	-67.2	-3.5
dilaurylphosphatidylethanolamine ^a	84	23	-100	2.3
calcium pyrophosphate				
(1)	75	-39	-69	-11.0
(2)	64	-24	-66	-8.0
sodium pyrophosphate anhydrate				
(1)	87	-33	-46	2.7
(2)	81	-27	-50	1.3
sodium pyrophosphate dodecahydrate				
(1)	76	-32	-49	-1.7
(2)	78	-26	-58	-2.0
sodium dihydrogen pyrophosphate anhydrate	65	-24	-80	-13.0
sodium tripolyphosphate ^d				
α	107	-24	-69	4.6
β	80	20	-117	-5.6
sodium ATP trihydrate				
α	79.4	8.3	-121.2	-11.2
β	69.9	10.2	-143.2	-21.0
γ	77.7	9.2	-110.3	-7.9
calcium ATP-DPA				
α	77.7	9.1	-125.4	-12.9
β	69.4	10.1	-142.8	-21.0
γ	77.6	-26.3	-76.7	-8.5
magnesium ATP-DPA				
α	83.8	9.6	-127.6	-11.4
β	71.6	12.1	-140.9	-19.0
γ	82.4	-25.6	-81.4	-8.2

^a Herzfeld, J.; Griffing, R. G.; Haberkorn, R. A. *Biochemistry* **1978**, *17*, 2711-2718. ^b Rothwell, W. P.; Waugh, J. S.; Yesinowski, J. P. *J. Am. Chem. Soc.* **1980**, *102*, 2637-2643. ^c Kohler, S. J.; Ellett, J. D.; Klein, M. P. *J. Chem. Phys.* **1976**, *50*, 4451-4452. ^d Burlinson, N. E.; Dunell, B. A.; Ripmeister, J. A. *J. Magn. Reson.* **1986**, *67*, 217-230. ^e Numbers in parentheses are used to distinguish different resonances arising from inequivalent nuclei and greek letters denote different positions on the same molecule. Chemical shifts are referenced against 85% H₃PO₄ with positive denoting downfield.

dehydrating the decahydrate at 130 °C to constant weight, which was equal to the theoretical weight for complete dehydration. The other simple phosphates were either used directly or washed with cold anhydrous ethanol to remove phosphoric acid contaminant.

Instrumentation. All spectra were recorded on a spectrometer of local design¹⁷ (109.298 MHz for ³¹P) using a Doty Scientific MASS probe. Pulses of 90° were typically 5 μs for both protons and phosphorus. Cross-polarized MASS (CP-MASS) spectra were taken under Hartmann-Hahn matched condition with a flip-back pulse¹⁸ at the end of each acquisition. Various cross-polarization times were used (0.5-2.0 ms). For simple Bloch decay experiments with proton decoupling, long repetition times were necessary due to long ³¹P T₁'s, approximately 24 s for NaATP. Sample spinning rates were typically 2.3-4.0 kHz. The rotor speeds were determined by an home-built optical tachometer fitted to the bottom of the stator. Static powder patterns were obtained in the same manner as MASS spectra without sample rotation. In addition, fully phased cycled chemical shift echo spectra were recorded to obtain accurate powder patterns.¹⁹

Recovery of Chemical Shift Tensors. The procedure for recovering chemical shift tensor elements was similar to the nonlinear least-squares

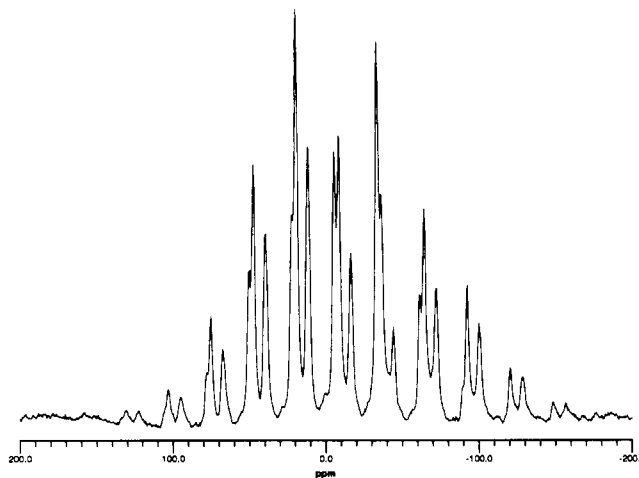


Figure 3. A 109.3-MHz ³¹P CP-MASS NMR spectrum of magnesium ATP-DPA, recorded by using a Hartmann-Hahn matched cross-polarization experiment. The sample was spun at 2.8 kHz. Chemical shifts are relative to 85% phosphoric acid. The proton decoupling field was 45 kHz. The spectrum was taken at 25 °C. The total number acquisitions was 500.

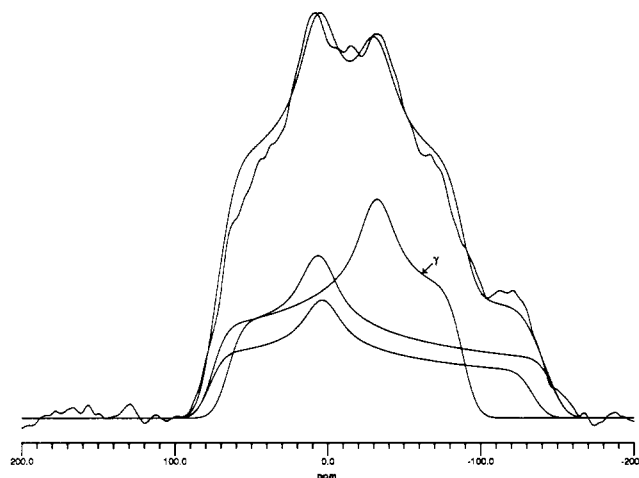


Figure 4. Comparison of the experimental 109.3-MHz ³¹P NMR powder pattern of the magnesium ATP-DPA complex with the spectrum calculated from the shift tensor elements listed in Table I. The powder pattern was taken by using a chemical shift echo experiment. The individual components of the calculated powder pattern are also shown. The proton decoupling field was 45 kHz. The spectrum was taken at 25 °C. The total number acquisitions was 1000.

analysis described by Herzfeld and Berger.¹¹ To ensure accurate intensities, the MASS sideband intensities were extracted by using NTCCAP, a spectrum simulation program, with an admixture of Lorentzian-Gaussian line shape. This method was especially useful for those spectra in which the resonances were not completely resolved as was the case for all ATP complexes studied. It is important to note that the isotropic shift is measured directly from the MASS spectrum.¹⁰ The isotropic frequencies were measured with respect to an 85% H₃PO₄ standard. The frequency of the standard was measured under conditions identical with those of the solid sample before and after each experiment.

Results and Discussion

The MASS spectrum of the MgATP-BPA complex shown in Figure 3 was typical of those used in this study. The three resonances, one from each of the three phosphorus nuclei of the chain, are clearly resolved. The chemical shift parameters obtained in the manner described above were used to calculate static powder pattern spectra, which in turn were compared to experimental ones. A comparison of the experimental nonspinning spectrum of MgATP-BPA with that calculated is shown in Figure 4. The agreement is very good and indicates that the chemical shift tensor elements obtained from the MASS spectra in the manner described above were accurate. The chemical shift tensor elements of a

(17) Shih, W. C.-W. Doctoral Thesis, University of California, Berkeley, 1979.

(18) Stekjalst, E. O.; Schaefer, J. *J. Magn. Reson.* **1975**, *18*, 560-562.

(19) Rance, M.; Byrd, R. A. *J. Magn. Reson.* **1983**, *52*, 221-240.

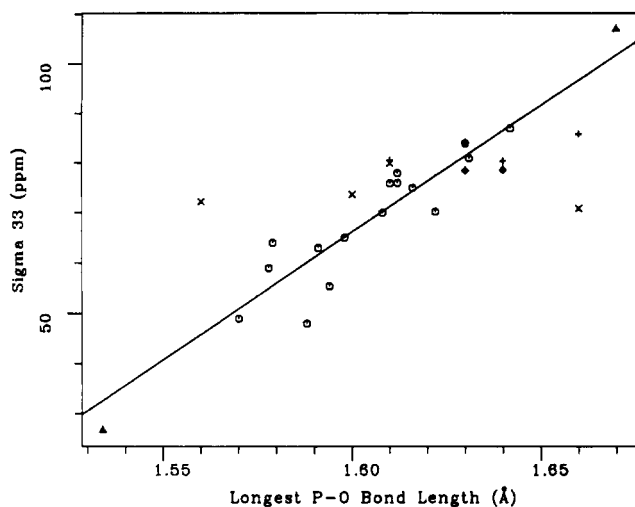


Figure 5. σ_{33} as a function of the longest P-O bond length: (Δ), urea-phosphoric acid complex and sodium triphosphate; (+), the α positions, (\times), the β positions, and (\diamond) the γ positions of the ATP complexes; (\circ), the remaining compounds listed in Table I. The best-fit line was determined by using the \circ points. The equation for this line is $\sigma_{33} = 499 \text{ \AA}^{-1} \text{ ppm} \times r - 731 \text{ ppm}$, where r is the bond length.

variety of phosphates and phosphate esters are tabulated in Table I. Included in this table are results obtained in our laboratory and those published elsewhere.^{12,13,20}

Isotropic Chemical Shifts. The solid-state isotropic ^{31}P chemical shift data differ in detail from those measured in solution. The variation in the isotropic shifts of the sodium, calcium, and magnesium hydrogen phosphates reflects the strength of acidic hydrogen bonds to the phosphate groups and cation dependencies.⁷ The upfield shift associated with the protonation observed in solution studies²¹ is not manifest in our MASS data. A counterion effect has recently been addressed by Turner.⁷ In that study, the isotropic chemical shift was found to be dependent on the electronegativity of the cation. This effect also is reflected in the data shown in Table I. Comparing the calcium to the sodium pyrophosphate, we observe that all three tensor elements, and therefore the isotropic chemical shift, of the calcium salt shift upfield relative to the sodium. This is consistent with a greater degree of electron withdrawal by the divalent cation and with the electronegativity term of eq 1. Beyond these qualitative observations, we found no other discernible trends in the isotropic chemical shift data. However, the individual tensor elements of these phosphates do form a consistent set of data with respect to their correlation to molecular structure and bonding. This is the subject of the following discussion.

Bond Length Correlations. The P-OR bond (where R = P, C, or H) of a phosphate ester is in most cases the longest of the four P-O bonds (see Table II). The R group effectively reduces the π -bond order of the P-OR bond. In general, the σ_{33} tensor element, the downfield extreme of the chemical shift tensor, lies in the same direction as longest P-O(1) bond (see Figure 2). When the magnitude of this tensor element was plotted as a function of the longest P-O bond length, a linear correlation was observed. This is shown in Figure 5. This relationship between the σ_{33} tensor element and bond lengths holds over a wide variety of phosphates. It accommodates the extreme 1.670-Å bond length of the terminal P-O bond of sodium triphosphate,⁸ chemical tensor values of which were determined recently by Burlinson.¹⁴ The urea-phosphoric acid complex, the shift tensor of which was determined by Herzfeld,¹³ also lies very close to the best-fit line. For this compound, we took into account the presence of an anomalously short hydrogen bond, as determined by neutron

Table II. Bond Lengths and Bond Angles of the Phosphates Used To Determine the Correlations Shown in Figures 5-9

compound	P-O bond length		bond angles	
	max	min ^a	O=P=O	ROPOR'
urea-phosphoric acid complex ^a	1.534	1.512	111.9	110.8
sodium hydrogen phosphate dodecahydrate ^b	1.594	1.514		
magnesium hydrogen phosphate trihydrate ^c (newberyite)	1.588	1.521		
calcium hydrogen phosphate dihydrate ^d (brushite)	1.608	1.511	109.0	104.3
calcium dihydrogen phosphate monohydrate ^e				
(1)	1.570	1.496	115.3	107.8
(2)	1.578	1.507	119.7	107.1
barium diethylphosphate ^f	1.61	1.52	121.6	103.5
sodium GMP heptahydrate ^g	1.622	1.511		
phosphorylethanolamine ^h	1.591	1.498	117.4	106.2
dilaurylphosphatidylethanolamine ⁱ	1.63	1.45	119	101
calcium pyrophosphate ^h				
(1)	1.616	1.505	114.8	105.3
(2)	1.579	1.493	113.4	106.4
sodium pyrophosphate anhydrate ⁱ				
(1)	1.642	1.512		
(2)	1.513	1.514		
sodium pyrophosphate dodecahydrate ^j	1.612	1.507		
sodium dihydrogen pyrophosphate hexahydrate ^k	1.598	1.493	117.7	104.5
sodium triphosphate ^l				
α	1.67	1.50		
β	1.61	1.49	116	99
sodium ATP trihydrate ^m				
α	1.61	1.51	122	101
β	1.66	1.52	122	98
γ	1.64	1.43		97
calcium ATP-DPA ⁿ				
α	1.64	1.54	116	101
β	1.56	1.51	117	108
γ	1.63	1.46		
magnesium ATP-DPA ⁿ				
α	1.66	1.51	117	101
β	1.60	1.45	121	104
γ	1.63	1.49		

^a Mootz, D.; Albrand, K.-R. *Acta Crystallogr.* **1972**, *B28*, 2459-2463. ^b Catti, M.; Ferraris, G.; Franchini-Angela, M. *Acta Crystallogr.* **1977**, *33*, 3449-3452. ^c Sutor, D. *J. Acta Crystallogr.* **1967**, *B23*, 418-422. ^d Curry, N. A.; Jones, D. W. *J. Chem. Soc. A* **1971**, 3725-3729. ^e Dickens, B.; Bowne, J. S. *Acta Crystallogr.* **1971**, *B27*, 2247-2255. ^f Herzfeld, J.; Griffin, R. G.; Haberkorn, R. A. *Biochemistry* **1978**, *17*, 2711-2718. ^g Katti, S. K.; Seshadri, T. P.; Viswamitra, M. A. *Acta Crystallogr.* **1981**, *B37*, 1825-1831. ^h Calvo, C. *Inorg. Chem.* **1968**, *7*, 1345-1351. ⁱ Leung, K. L.; Calvo, C. *Can. J. Chem.* **1972**, *50*, 2519-2526. ^j McDonald, W. S.; Cruickshank, D. W. *J. Acta Crystallogr.* **1967**, *22*, 43-48. ^k Collin, R. L.; Willis, M. *Acta Crystallogr.* **1971**, *B27*, 291-302. ^l Cruickshank, D. W. *J. Chem. Soc.* **1961**, 5486-5504. ^m Kennard, O.; Isaacs, N. W.; Motherwell, W. D. S.; Coppola, J. C.; Wampler, D. L.; Larson, A. C.; Watson, D. G., *Proc. R. Soc. London* **1971**, *325A*, 401-436. ⁿ Cini, R.; Burla, M. C.; Nunzi, A.; Polidori, G. P.; Zanazzi, P. F. *J. Chem. Soc., Dalton Trans.* **1984**, 2467-2476. ^o The minimum bond parameter is the average of the two shortest P-O bonds.

diffraction,²² to one of the oxygens in σ_{11} - σ_{22} plane. Similar to protonation, such a strong hydrogen bond would necessarily influence the P-O $d_{\text{P-O}}$ π bond.⁸ Herzfeld¹³ found the orientation of the σ_{33} element for this complex to be significantly different from that found for barium diethylphosphate. Unlike most cases, the tensor element was tilted significantly away from the longest P-O bond. To account for these observations, we averaged the length of the longest P-O bond with that of the P-O(3) bond,

(20) Rothwell, W. P.; Waugh, J. S.; Yesinowski, J. P. *J. Am. Chem. Soc.* **1980**, *102*, 2637-2643.

(21) Gadian, D. G.; Radda, G. K.; Richards, R. E.; Seeley, P. J. In *Biochemical Applications of Magnetic Resonance*; Schulman, R. G., Ed.; Academic Press: New York, 1979; pp 463-536.

(22) Kostansek, E. C.; Busing, W. R. *Acta Crystallogr.* **1972**, *B28*, 2454-2459.

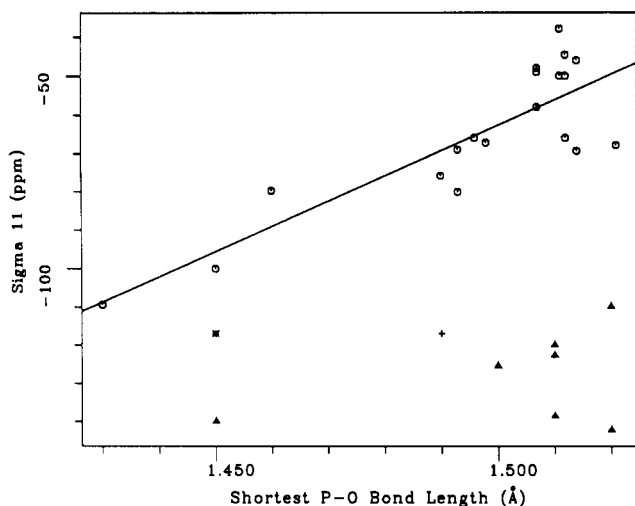


Figure 6. σ_{11} as a function of the average of the two shortest P-O bond lengths which both lie on the plane formed by σ_{11} and σ_{22} : (Δ) the α and β positions of the three ATP complexes and the barium diethylphosphate; (\times and $*$) sodium triphosphate, experimental and predicted, respectively (see text for details); (\circ) the remaining compounds listed in Table I. The best-fit line was determined by using only \circ points. The equation for this line is $\sigma_{11} = 629 \text{ \AA}^{-1} \text{ ppm} \times r - 1050 \text{ ppm}$, where r is the bond length.

as denoted in Figure 2, to obtain a value of 1.534 Å, which yielded a better agreement with the σ_{33} maximum bond length correlation. As can be seen in Figure 5, two σ_{33} bond length points deviate significantly from the best-fit line, those corresponding to the β positions of both the calcium and sodium ATP complexes. By contrast, values for the β -magnesium ATP complex and sodium triphosphate tensor lie close to the line. Those points arising from β positions of triphosphate chains appear to form a separate group, which is characterized by the independence of their σ_{33} tensor element on the maximum bond length.

Since variations in bonding are not expected to be isolated along one direction, the relationship between the σ_{11} tensor element and the shortest P-O bond lengths was examined. A review of single-crystal studies^{12,13} showed that the σ_{11} tensor element is approximately coplanar with the two shortest bonds and directed in the manner shown in Figure 2. The lengths of these short bonds are restricted to a small range with most falling between 1.48 and 1.52 Å. Hence, the variation in $d_{\text{P-O}} \pi$ -bond order for these bonds was also expected to be small. Figure 6 is a plot of magnitude of the σ_{11} tensor element as a function of the average of the two shortest P-O bond lengths. Because of the small range in bond lengths, it was difficult to discern any trends. However, if the data points corresponding to phosphate groups of the type PO-P-OP and PO-P-OC are ignored, a linear trend is apparent. The existence of such a linear behavior is tenuous since it depends on three unusually short P-O bonds. However, it is noteworthy that the slope of the linear least-squares fit of the σ_{11} shortest bond data is similar in value to that of the σ_{33} longest bond fit. These two bond-length correlations taken together are consistent with the previously reported linear relationship between chemical shift anisotropy and P-O bond length described by Grimmer.⁶

A reason why PO-P-OP type groups do not follow the observed trend is suggested by the following observations. On the basis of the $d_{\text{P-O}} \pi$ -bond order of the β -position P-O bond of sodium triphosphate, Cruickshank⁸ predicted a P-O bond length of about 1.45 Å compared to the crystallographic value of 1.49 Å. This predicted value is much closer to the value one would expect on the basis of the least-squares fit shown in Figure 6. The O-P-O bond angle of 99° for the triphosphate is an extreme departure from 109.5°, the unperturbed sp^3 bond angle. On the basis of this small bond angle, Cruickshank⁸ argued that the σ bonding in the triphosphate must be significantly different. In such cases, variations in shift tensor elements would not be expected to be solely related to changes in $d_{\text{P-O}} \pi$ -bond order. Hence, chemical shift correlations to changes in bond lengths would not yield simple

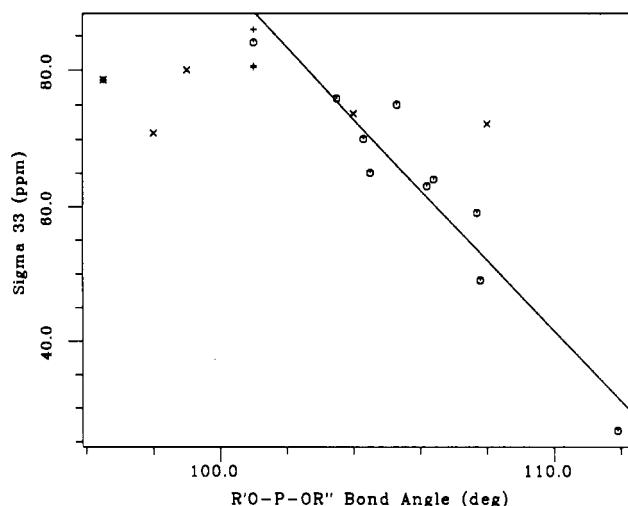


Figure 7. σ_{33} as a function of the R'O-P-OR'' bond angle: (+) the α position and (\times) the β positions of the ATP complexes; ($*$) the POPOH angle of the γ position of the sodium ATP complex; (\circ) the remaining compounds listed in Table II. The best-fit line was determined using only the \circ points. The equation for this line is $\sigma_{33} = -4.24 \text{ deg}^{-1} \text{ ppm} \times \theta + 511 \text{ ppm}$, where θ is the bond angle.

results. This argument can be generalized to the other diesters such as the α -ATP positions, which all have PO-P-OC bond angles of 101°. Cation effects such as those described by Turner⁷ may also contribute to the deviation. Such effects explain why the data point for barium diethylphosphate deviates significantly from the least-squares line. Barium has both a significantly larger ionic radius and lower electronegativity than do the other cations encountered in this study.⁹

Bond Angle Correlations. To test bond angle hybridization effects, we investigated the variations of the σ_{33} and σ_{11} values with changes in the appropriate bond angles (see Figure 2). For the σ_{33} case, the O-P-C bond angle that is coplanar with the σ_{33} - σ_{22} plane was considered. Similarly, variation in the σ_{11} tensor element as function of the O-P-O bond angle that lies on the plane formed by the σ_{11} and σ_{22} was investigated. Figure 7 relates the magnitudes of the σ_{33} elements to the appropriate bond angles. Again, a reasonably linear behavior was observed. The values for the β positions of sodium and calcium ATP, as well as that of β -sodium triphosphate, deviated significantly from the observed trend. In a situation similar to the bond length correlation discussed earlier, the tensor values of these triphosphates are independent of bond angle. Finally, the σ_{11} elements were plotted as a function of the bond angles formed by the two nonester P-O bonds (Figure 8). A monotonic trend was observed. We see, as in the bond length correlation (Figure 6), that the six α - and β -ATP values seem to follow no trend. These bond angle-chemical shift observations are consistent with those previously reported by others.^{4,7} The chemical shift anisotropy-bond angle plots of our data, similar to those constructed by Turner,⁷ also exhibited a linear trend although with considerably more scatter. It was gratifying to note that the chemical shift tensor values obtained by Dutasta⁴ for thioxophosphonates follow a σ_{33} -bond angle relationship, in addition to the chemical shift anisotropy-bond angle noted by the author. This suggests that the linear trends that we have observed may be common to other types of phosphorus compounds.

The linearity of both the σ_{33} -bond length and σ_{33} -bond angle correlations suggested that the R'O-P-OR'' bond angles must be linearly related to P-OR bond lengths. Figure 9 clearly demonstrates this point. The bond angles and corresponding longest bond lengths are indeed linearly correlated to each other. Since P-O bond lengths are linear functions of their $d_{\text{P-O}} \pi$ -bond order,⁸ we conclude that the R'O-P-OR'' bond angle of a phosphate ester and the $d_{\text{P-O}} \pi$ -bond order of the P-OR bond must also be related. Two potential explanations for this phenomenon are the following. First is that the $d_{\text{P-O}} \pi$ bonds result from "back bonding" of the p oxygen orbital electrons into the

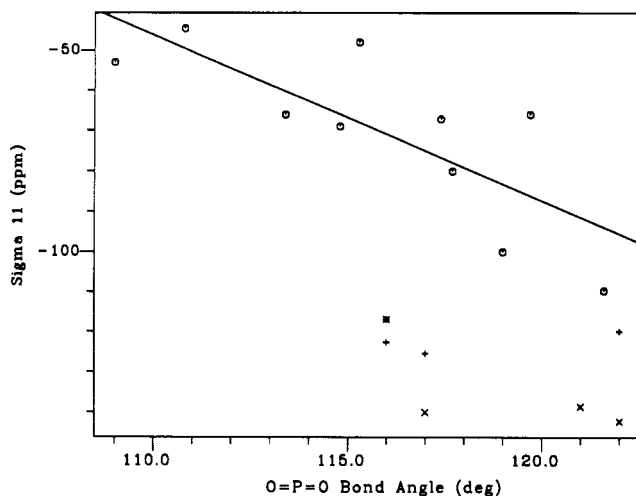


Figure 8. σ_{11} as a function of the O=P=O bond angle: (+) the α position and (x) the β positions of the ATP complexes; (*) β position of the sodium triphosphate; (O) the remaining compounds listed Table II. The best-fit line was determined by using only the O points. The equation for this line is $\sigma_{11} = -4.11 \text{ deg}^{-1} \text{ ppm} \times \theta + 406 \text{ ppm}$, where θ is the bond angle.

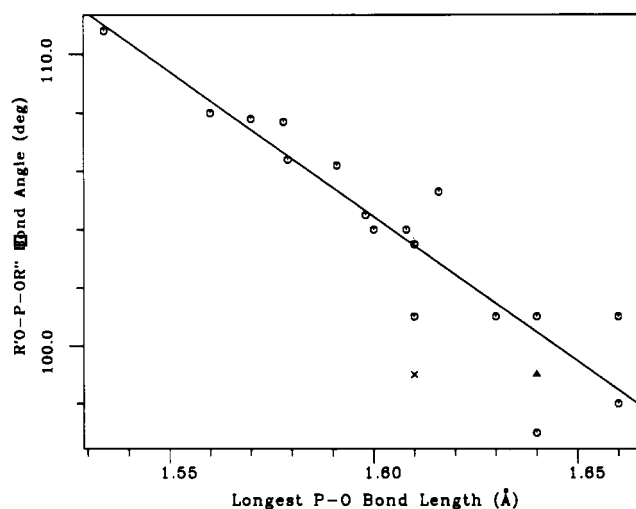


Figure 9. R'O-P-OR'' bond angle as a function of the longest P-O bond length: (x) and Δ sodium triphosphate, experimental and predicted, respectively, and (O), the remaining compounds listed Table II. The best-fit line was determined by using only the O points. The equation for this line is bond angle = $99.4 \text{ deg } \text{\AA}^{-1} \times \text{bond length} + 263^\circ$.

empty phosphorus d orbitals.⁹ Hence, any PO-R ester "Bonds will reduce the $d_{\text{P}}-p_{\text{O}}$ orbital interactions with concomitant P-O bond elongation. The angle between the nonester P-O bonds, which possess their full π character, will thus increase to reduce bond-bond repulsion. Alternatively, as suggested by Cruickshank⁸ and discussed above, the observed variations in bond length and angle are due to changes in the σ bonding. The R'-O-P-OR'' bond angles for phosphates listed in Table II suggest the P-OR bonds are essentially sp^3 hybridized. The greatest departure from this hybridization is observed for the β position of sodium triphosphate and sodium ATP and the α position of all three ATP complexes. The bond angle for these phosphate groups range from 101° to 98° , which corresponds to a hybridization half-way between sp^3 and sp^3d^2 . For these cases, the change in hybridization would result in the P-O π -bond order being the smallest and the P-O bond longest (see Figure 8). Regardless of the exact nature, the presence of bond length-bond angle relationships clearly indicates that π -bond order and bond angle effects cannot be separated.

Similar bond length-bond angle correlations were also found for other phosphorus compounds. A review of the structural data of four compounds POX_3 (where X = F, Cl, Br, and methyl), the

same compounds studied by Grimmer,^{6,23-25} shows that linear correlations exist between the P-O bond length and both O-P-X and X-P-X bond angle, except in the case of the bromine compound. The structural data for this latter compound are somewhat questionable with a quoted P-O bond length error of $\pm 0.1 \text{ \AA}$.²⁵ The presence of bond length-bond angle relationships in these compounds is encouraging and suggests that the link between π -bond order and bond angle may be general for a wide variety of phosphoryl derivatives.

A similar bond length and angle correlation was not observed among the nonester P-O bonds (PO(3) and PO(4) bonds in Figure 2) in phosphate esters. The large scatter in the σ_{11} correlations suggested that such a relationship between bond lengths and bond angles was unlikely. It is somewhat perplexing that such a correlation exists in one direction and not in the other. One possible explanation is that the π -bond character of these nonester P-O bonds is relatively unchanged and affected only indirectly by the presence of neighboring ester bonds, as suggested by the observation that the lengths of most of these P-O bonds lie in a small range. In many cases, metal interactions are expected to be the strongest among these nonester oxygens. This would also explain why σ_{11} values correlate so poorly with bond angles and bond lengths.

From these observations we conclude that the σ -bond order and bond angle terms in eq 1 are not totally independent of each other and interpretation of ^{31}P chemical shifts of phosphates must be cautious. Given the existing correlations between P-O bond lengths and π -bond order, in addition to the linear trends between chemical shift tensor elements and bond lengths, it is tempting to conclude that the phosphorus chemical shift interaction, at least in the case of phosphates, is dependent on the degree of $d_{\text{P}}-p_{\text{O}}$ π bonding. However, as pointed out earlier, a σ bond/hybridization effect cannot be discounted. In reality, the effects may be related and cannot be simply separated. Exceptions to the observed trends indicate that other influences such as metal interactions are important in some cases.

Formal Charge Effects on σ_{22} . We have conspicuously omitted discussion about the σ_{22} principal values of the phosphorus chemical shift tensors. The σ_{22} elements exhibited no discernible correlation with any bond lengths or angles. However, σ_{22} seems to be sensitive to the formal charge of the phosphate group. From Table I, it can be seen that the diesters and the doubly protonated simple phosphates form a group shifted significantly downfield in the region 1-25 ppm. The monoesters fall in a region from -12 to -40 ppm.

Conclusion

We have studied a wide variety of phosphate-bearing compounds in the solid phase using ^{31}P magic-angle sampling spinning. Although the data set is limited due to the naturally small variation in structure, there seems to be a good correlation between P-OR bond length and the downfield extremum of the chemical shift powder pattern. The simultaneous linear dependence on both bond lengths and angles suggest that interpretations of ^{31}P chemical shifts based on eq 1 must be carried out with caution. Equation 1 with respect to the σ_{33} tensor element reduces to a single-term equation. Our study indicates in the solid state that chemical shift interactions are dominated by $d_{\text{P}}-p_{\text{O}}$ π -bonding effects. In the case of the σ_{11} tensor element, counterions play a significant role in addition to P-O π bonding. The σ_{22} component does not correlate well with any structural variations. However, it seems to be sensitive to the overall charge of the phosphate group.

Acknowledgment. We thank Dr. J. Herzfeld for providing the calculated sideband intensity data on which the analyses are based. This work was supported by the Assistant Secretary for Environment, Office of Environmental Research and Development, Biomedical and Environmental Research Division, U.S. Department of Energy under Contract DE-AC03-76SF00098.

(23) Wang, H. *Acta Chem. Scand.* **1965**, *19*, 879-882.

(24) Moritani, T.; Kozo, K.; Morino, Y. *Inorg. Chem.* **1971**, *10*, 344-350.

(25) Secrist, J. H.; Brockway, L. O. *J. Am. Chem. Soc.* **1944**, *19*, 1941-1946.